A SUPERMASSIVE BLACK HOLE FUNDAMENTAL PLANE FOR ELLIPTICALS

SUDHANSHU BARWAY AND AJIT KEMBHAVI

Inter-University Centre for Astronomy and Astrophysics, Post Bag 4, Ganeshkhind, Pune 411 007, India; sudhan@iucaa.ernet.in, akk@iucaa.ernet.in

ABSTRACT

We obtain the coefficients of a new fundamental plane for supermassive black holes at the centers of elliptical galaxies, involving measured central black hole mass and photometric parameters that define the light distribution. The galaxies are tightly distributed around this mass fundamental plane, with improvement in the rms residual over those obtained from the M_{BH}-σ and M_{BH}-L relations. This implies a strong multidimensional link between central massive black hole formation and global photometric properties of elliptical galaxies, and provides an improved estimate of black hole mass from galaxy data.

Subject headings: black hole physics — galaxies: elliptical and lenticular, cD — galaxies: evolution — galaxies: fundamental parameters — galaxies: kinematics and dynamics — galaxies: nuclei

1. INTRODUCTION

The existence of massive black holes (BHs) at the center of nearby inactive galaxies, as well as in the nuclei of active galaxies and in quasars, is well established. Observations based on high-resolution data and reverberation mapping are now available, which allow measurement of the masses of BH using different techniques (Ferrarese & Ford 2005; Metzroth et al. 2006; Shapiro et al. 2006). Kormendy & Richstone (1995) showed that the measured BH mass, M_{BH}, is correlated with the bulge luminosity, L, and bulge mass, M_{bulge}, with rms scatter ∼0.5 dex in log M_{BH} (see also Magorrian et al. 1998). A tight correlation between M_{BH} and the central velocity dispersion σ of the host galaxy, with smaller rms scatter of ∼0.34 dex in log M_{BH}, was reported by Ferrarese & Merritt (2000) and Gebhardt et al. (2000); however, the published estimates of slope in the M_{BH}-σ relation span a wide range (3.75–5.30; see Tremaine et al. 2002). The small scatter of the M_{BH}-σ relation suggests that the bulge dynamics (or mass), rather than the luminosity, is responsible for the tight correlation.

It is believed that massive black holes play an important role in the formation and evolution of galaxies, and the growth of the BH and bulges must be linked to the same physical processes; this results in BH masses that are related to the properties of host galaxies (Silk & Rees 1998; Haehnelt & Kauffmann 2000; Adams et al. 2001; Merritt & Poon 2004; Sazonov et al. 2005). Graham et al. (2001) and Marconi & Hunt (2003) have shown that when bulge parameters are measured with sufficient accuracy using the technique of bulge-disk decomposition, the resulting scatter in the M_{BH}-L relation is comparable to that in the M_{BH}-σ relation (see also Graham 2007). Marconi & Hunt (2003) also suggested that a combination σ and bulge effective radius, r_e should be used to derive the correlations between M_{BH} and other bulge properties. Recently, Lauer et al. (2006) have suggested that the bulge luminosity may be a better indicator of BH mass than the bulge velocity dispersion at the high-mass end for brightest cluster galaxies. However, in spite of all these attempts, our understanding of how the photometric properties of galaxies and their central BHs are linked in the process of formation of galaxies remains unclear.

In this Letter, we show that log M_{BH}, log r_e, and $\langle \mu_b(<r_e) \rangle$, which is the mean bulge surface brightness in magnitude within r_e, are tightly correlated for nearby elliptical galaxies with measured central BH masses. The scatter around the best-fit plane

is significantly less than the scatter in various two-dimensional relations. It is also less than the scatter obtained if BH masses are estimated from the photometric parameters of galaxies using the standard fundamental plane for ellipticals and the M_{BH}-σ relation. In § 2 we provide details about the samples of galaxies used in the analysis. We present the results in § 3, a discussion in § 4, and in § 5 a summary of the work. Throughout this Letter, we use $H_0 = 70$ km s^{-1} Mpc^{-1}, and express r_e in kiloparsecs, σ in units of km s^{-1}, and mass and luminosity in solar units.

2. THE DATA

To obtain the photometric scaling relation, we have considered a sample of 20 galaxies classified as elliptical in the Ferrarese & Ford (2005) galaxy list with measured black hole masses. In Table 1 we report the relevant data for this sample. To compare the estimates of central black hole masses obtained from our planar relation and the M_{BH}-σ and M_{BH}-L relations, we consider a sample of 22 elliptical galaxies from the Coma Cluster. This sample was observed by Jørgensen et al. (1992) in the Johnson B band; a description of the data and the global parameters obtained from the images can be found in that work.

3. A NEW FUNDAMENTAL PLANE FOR NEARBY ELLIPTICALS

The M_{BH}-σ and M_{BH}-L relations offer two ways to estimate the BH mass from other galaxy properties, and have been applied to AGNs (McLure & Dunlop 2002), BL Lac objects (Falomo et al. 2002), low-redshift radio galaxies (Bettoni et al. 2003), and bright cluster galaxies (Lauer et al. 2006; Batcheldor et al. 2006). We have revisited the M_{BH}-σ relation and M_{BH}-L relation by applying a bisector linear regression fit (Akritas & Bershady 1996) to the data given in Table 1 for the sample of nearby elliptical galaxies with measured BH masses. The two best-fit relations are

$$\log M_{BH} = (4.53 \pm 0.49) \log \sigma - (2.24 \pm 1.17), \quad (1)$$

$$\log M_{BH} = -(0.56 \pm 0.06)L_B - (3.10 \pm 1.51). \quad (2)$$

The rms scatter around the best-fit lines above is 0.34 and 0.42 dex, respectively, along the log M_{BH} axis. Both the relations are in good agreement with those in Bettoni et al. (2003)

TABLE 1
BASIC PARAMETERS FOR ELLIPTICAL GALAXIES WITH MEASURED BLACK HOLE MASS

Object	Type	Distance (Mpc)	M_{BH} ($M_\odot$)	σ (km s^{-1})	L_B (mag)	log r_e (kpc)	$\langle\mu_b(<r_e)\rangle$ (mag arcsec^{-2})
NGC 221/M32	−6.0	0.80	$2.5^{+0.5}_{-0.5} \times 10^6$	75 ± 10	−15.80 ± 0.18	−0.83	18.69
NGC 821	−5.0	24.1	$3.7^{+2.4}_{-0.8} \times 10^7$	209 ± 26	−20.42 ± 0.21	0.72	21.85
NGC 2778	−5.0	22.9	$1.4^{+0.8}_{-0.9} \times 10^7$	175 ± 22	−18.58 ± 0.33	0.26	21.38
NGC 3377	−5.0	11.2	$1.0^{+0.9}_{-0.1} \times 10^8$	145 ± 17	−19.18 ± 0.13	0.26	20.76
NGC 3379	−5.0	10.6	$1.0^{+0.6}_{-0.5} \times 10^8$	206 ± 26	−19.81 ± 0.20	0.26	20.16
NGC 3608	−5.0	22.9	$1.9^{+1.0}_{-0.6} \times 10^8$	182 ± 27	−20.07 ± 0.17	0.59	21.41
NGC 4261	−5.0	31.6	$5.2^{+1.0}_{-1.1} \times 10^8$	315 ± 38	−21.23 ± 0.20	0.77	21.25
NGC 4291	−5.0	26.2	$3.1^{+0.8}_{-2.3} \times 10^8$	242 ± 35	−19.72 ± 0.35	0.27	20.25
NGC 4374/M84	−5.0	18.4	$1.0^{+2.0}_{-0.6} \times 10^9$	296 ± 37	−21.40 ± 0.31	0.68	20.81
NGC 4473	−5.0	15.7	$1.1^{+0.4}_{-0.8} \times 10^8$	190 ± 25	−19.86 ± 0.14	0.28	20.19
NGC 4486/M87	−4.0	16.1	$3.4^{+1.0}_{-1.0} \times 10^9$	375 ± 45	−21.71 ± 0.16	0.91	21.60
NGC 4564	−5.0	15.0	$5.6^{+0.3}_{-0.8} \times 10^7$	162 ± 20	−18.94 ± 0.18	0.19	20.64
NGC 4697	−5.0	11.7	$1.7^{+0.2}_{-0.1} \times 10^8$	177 ± 10	−20.20 ± 0.18	0.63	21.41
NGC 4649/M60	−5.0	16.8	$2.0^{+0.4}_{-0.6} \times 10^9$	385 ± 43	−21.30 ± 0.16	0.78	21.10
NGC 4742	−5.0	15.5	$1.4^{+0.4}_{-0.5} \times 10^7$	90 ± 05	−19.03 ± 0.10	−0.06	19.36
NGC 5845	−5.0	25.9	$2.4^{+0.4}_{-1.4} \times 10^8$	234 ± 36	−18.92 ± 0.25	−0.30	18.38
NGC 7052	−5.0	71.4	$4.0^{+2.8}_{-1.6} \times 10^8$	266 ± 34	−21.43 ± 0.38	0.89	22.01
IC 1459	−5.0	29.2	$1.5^{+1.0}_{-1.0} \times 10^9$	340 ± 41	−21.45 ± 0.32	0.73	20.81
NGC 6251	−5.0	107.0	$6.1^{+2.0}_{-2.1} \times 10^8$	290 ± 39	−21.95 ± 0.28	1.31	...
Cyg A	−5.0	240.0	$2.9^{+0.7}_{-0.7} \times 10^9$	270 ± 90	−20.03 ± 0.27	...	...

NOTE.—Cols. (1) and (2) give the name and the morphological type from RC3; col. (3) the distance, derived from surface brightness fluctuations (SBF; Tonry et al. 2001); cols. (4)–(6) provide the adopted values for the mass of black hole M_{BH}, velocity dispersion and absolute bulge luminosity L in B band (from Ferrarese & Ford 2005); cols. (7) and (8) give the effective radius r_e (from Faber et al. [1989] and using the distance in col. [3]) and mean surface brightness within effective radius in B band (from Faber et al. 1989).

and reference therein, but the relations are different from those of Ferrarese & Merritt (2000) and Gebhardt et al. (2000), as we have used a sample of nearby ellipticals only. It is possible that some of the scatter seen in the M_{BH}-σ and M_{BH}-L relations is caused by the effect of a third parameter. This is supported by the strong correlation that we find between log M_{BH} and log r_e, with a correlation coefficient $r = 0.89$, which is significant at the 99.99% confidence level for 19 objects; Marconi & Hunt (2003) have obtained a similar result.

Our aim is to derive a planar relation involving the BH mass and the basic photometric parameters r_e and $\langle\mu_b(<r_e)\rangle$; this can be used to estimate the black hole mass when it is not known from measurement, without reference to a spectroscopically

measured quantity such as the central velocity dispersion. We find that the least scatter around the best-fit plane in the space of the three parameters is obtained by expressing it in the form log $r_e = a$ log $M_{BH} + b\langle\mu_b(<r_e)\rangle +$ constant. We minimize the sum of the absolute residuals perpendicular to the plane, excluding one galaxy, NGC 4742, which is an outlier we have identified in Figure 1. The equation of the best-fit mass fundamental plane is

$$\log r_e = (0.32 \pm 0.06) \log M_{BH}$$
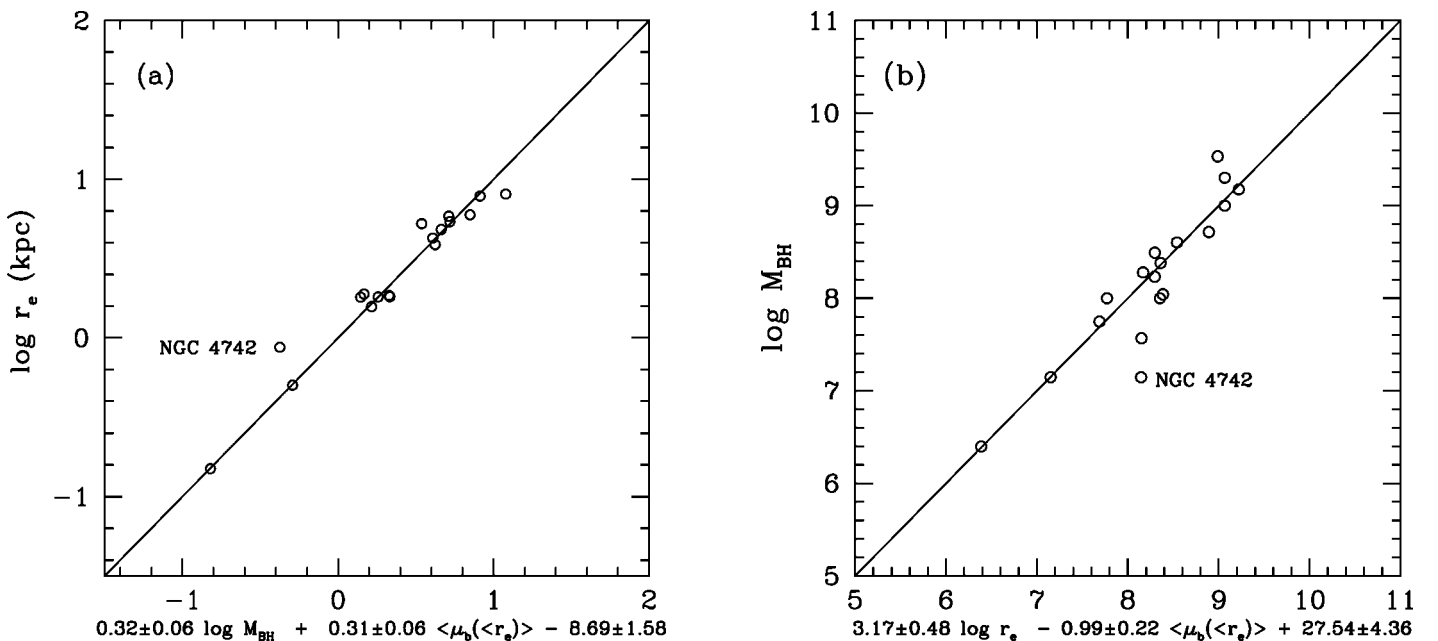$$+ (0.31 \pm 0.06)\langle\mu_b(<r_e)\rangle - 8.69 \pm 1.58. \quad (3)$$

FIG. 1.—Edge-on views of the mass fundamental plane relations for nearby ellipticals: (a) along one of the shorter axes of the plane, log r_e, and (b) along another axis of the plane, log M_{BH}.

The uncertainties on the mass FP coefficients were determined using a bootstrap method. An edge-on view along $\log r_e$ of the plane is shown in Figure 1a. The rms scatter in the direction of $\log r_e$ is 0.061 dex. Figure 1b shows another edge-on view of mass FP in the direction of $\log M_{BH}$, with rms scatter in that direction of 0.19 dex, which is significantly less than the scatter in the M_{BH}-σ relation (Gebhardt et al. 2000; Ferrarese & Merritt 2000). The outlier NGC 4742 is 6.32 × (rms scatter) from the plane along the $\log r_e$ axis. We have also obtained the equation of the best-fit plane including this outlier. The rms scatter then increases to 0.078 dex in $\log r_e$ and 0.25 dex along the $\log M_{BH}$ axis, respectively. Therefore, even with the outlier included, we have less scatter than in the $\log M_{BH}$–$\log \sigma$ and $\log M_{BH}$–$\log L$ fits.

If we exclude from the fit the four galaxies NGC 821, NGC 2778, NGC 4649, and NGC 7052, for which the BH sphere of influence is not resolved, and the outlier from the fit, the rms scatter in $\log M_{BH}$ around the best-fit plane obtained using the remaining 14 galaxies decreases to 0.17 dex.

For nearby ellipticals, we have derived the standard fundamental plane relation, using the same technique as in the case of the mass fundamental plane, and again excluding the outlying data point NGC 4742. The equation of the best-fit FP is

$$\log r_e = (1.34 \pm 0.22) \log \sigma$$
$$+ (0.30 \pm 0.05)\langle \mu_b(<r_e)\rangle - 8.93 \pm 0.74. \quad (4)$$

The rms scatter is 0.068 dex in $\log r_e$. The FP coefficients and rms scatter around the fit are in agreement with those available in the literature (Jørgensen et al. 2006).

4. DISCUSSION

As suggested by Ferrarese & Ford (2005), given the photometric parameters of an elliptical galaxy, the central velocity dispersion σ can be derived using the FP relation given in equation (4), if it is not directly observed, and then the M_{BH}-σ relation in equation (1) can be used to estimate the BH mass. However, the error in the estimated BH mass will then be the cumulative error of these two relations, thus increasing the uncertainty in the mass estimate. Another disadvantage of this approach is that the slope in the M_{BH}-σ relation spans the range 3.75–5.3, leading to further uncertainty in the estimate of the mass. The mass FP provides an improvement over this two-step procedure, and also helps to constrain the slope of the M_{BH}-σ relation, as described below.

We consider a two-dimensional relation of the form $\log M_{BH} = \alpha \log \sigma + \beta$, where α and β are constants to be determined. Introducing this into equation (4) for the fundamental plane, we get a plane in the space of $\log M_{BH}$, $\log r_e$, and $\langle \mu_b(<r_e)\rangle$, with the direction normal to the plane dependent on the value of α. In Figure 2 we have plotted, as a solid line, the angle between this normal and the normal to the mass FP in equation (3), for a range of values of α. The filled circles on the curve indicate the angles corresponding to specific values of α found in the literature, obtained by various groups from their fits to the data (see Tremaine et al. 2002). It is seen from the figure that the angle between the two planes is at a minimum near $\alpha = 4.5$, which should be the value to be used in the $\log M_{BH}$–$\log \sigma$ relation to determine black hole mass from the central dispersion velocity. The best fit in equation (1) corresponds to $\alpha = 4.53$. It will be interesting to see how the
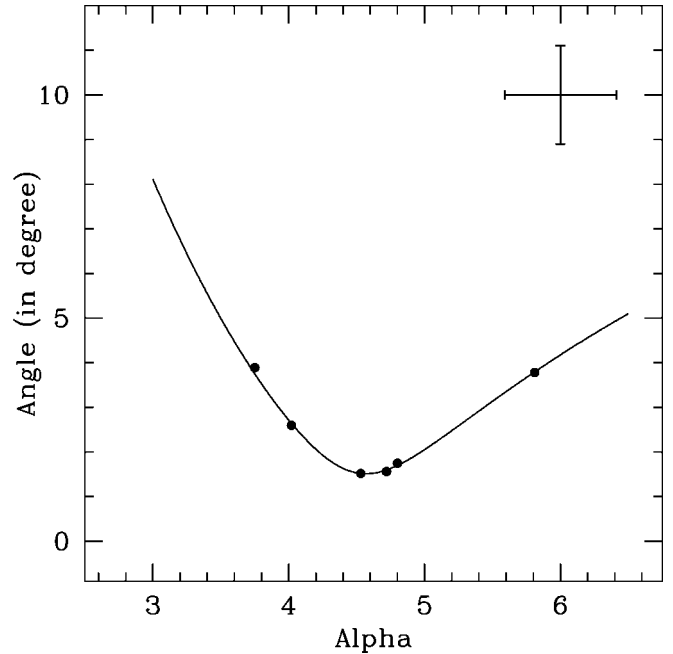

FIG. 2.—Curve shows the angle between the best-fit mass FP, and the plane derived using the fundamental plane in eq. (4) and the relation $M_{BH} = \alpha \log \sigma + \beta$ for a range of values of α. The filled circles indicate the angle for actual values of α taken from the literature (see Tremain et al. 2002). The typical error in the measured values of α and the derived angle between the planes is shown at the top right in the plot.

minimum value of α depends on the morphological type of the host galaxy.

We have used the mass FP to predict the black hole mass for a set of 22 elliptical galaxies from the Coma Cluster, using photometric data from Jørgensen et al. (1992). We have also obtained the black hole mass for these galaxies using equations (1) and (2). The masses obtained in these various ways are compared in Figure 3. It is seen from Figure 3a that the agreement between M_{BH}(mass FP) and $M_{BH}(\sigma)$ is good; the points are distributed around a line with slope close to unity, with a correlation coefficient $r = 0.93$, which is significant at better than the 99.9% level. A larger number of points will be needed for a better comparison and to examine any departures from linearity. The slope in the $\log M_{BH}$–$\log \sigma$ relation in equation (1) is close to the minimum value of α obtained from Figure 2. Using any other value of α will produce a less favorable comparison. We see from Figure 3b that M_{BH}(mass FP) and $M_{BH}(L)$ are distributed along a straight line with slope less than unity; for $M_{BH} \lesssim 10^{8.5} M_\odot$, masses obtained from the FP would be systematically less than masses obtained from the $\log M_{BH}$–$\log L$ relation. The dispersion of the points around the best-fit line is greater in this case than in Figure 3a. For completeness, in Figure 3c we also compare black hole masses obtained from the $\log M_{BH}$–$\log \sigma$ and $\log M_{BH}$–$\log L$ relations, and find a slope greater than unity and larger dispersion than in the other cases.

The three-dimensional mass FP has smaller rms deviation than in the earlier two-dimensional relations; while some reduction in residuals is expected when the number of parameters in the fit is increased from two to three, it appears that the process cannot be taken any further. We have considered a four-dimensional plane with the dispersion velocity σ included in the fit along with the two photometric parameters. However, we find that the residuals from the three-dimensional plane are not correlated with $\log \sigma$, and the quality of a four-dimensional fit involving $\log M_{BH}$, $\log r_e$, $\langle \mu_b(<r_e)\rangle$, and $\log \sigma$ is poor. A
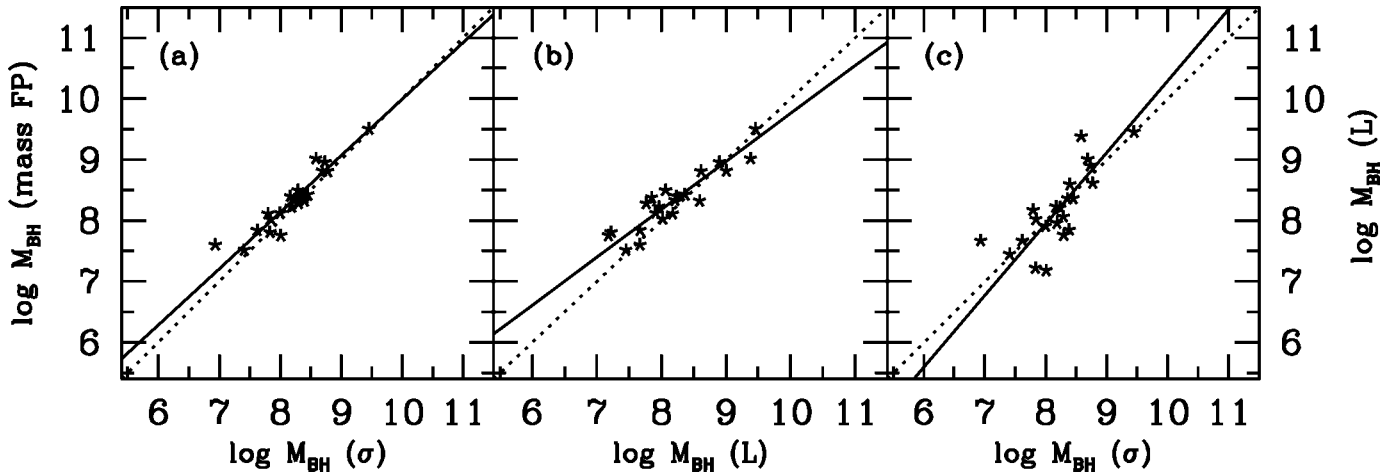
Fig. 3.—Comparison of black hole mass estimated using the mass fundamental plane, M_{BH}(mass FP), with (*a*) the mass $M_{BH}(\sigma)$ estimated using eq. (1) and $M_{BH}(\sigma)$ and (*b*) with the mass $M_{BH}(L)$ estimated using eq. (2). In (*c*) we compare $M_{BH}(\sigma)$ with $M_{BH}(L)$. In each panel the solid line indicates the linear fit to the points shown, while the dashed line has slope unity.

three-dimensional relation is therefore the best we can do with the available data.

It will be interesting to obtain the mass FP for photometric data in the near-infrared bands, since stellar population metallicity effects are less important than in the optical region (Pahre et al. 1998). Another issue to examine is whether the bulges of galaxies of various morphological types share a common mass FP.

5. SUMMARY

We have shown that log r_e, log M_{BH}, and $\langle \mu_b(<r_e) \rangle$ for nearby elliptical galaxies having measured central BH masses are tightly distributed about a plane with an rms scatter of 0.19 dex along

log M_{BH}. The scatter decreases to 0.17 dex in log M_{BH} when we use only those galaxies for which the BH sphere of influence is resolved. The mass FP provides a convenient way for estimating BH mass from photometric data alone.

REFERENCES

Adams, F. C., Graff, D. S., & Richstone, D. O. 2001, ApJ, 551, L31
Akritas, M. G., & Bershady, M. A. 1996, ApJ, 470, 706
Batcheldor, D., Marconi, A., Merritt, D., & Axon, D. J. 2006, preprint (astro-ph/0610264)
Bettoni, D., Falomo, R., Fasano, G., & Govoni, F. 2003, A&A, 399, 869
Faber, S. M., et al. 1989, ApJS, 69, 763
Falomo, R., Kotilainen, J. K., & Treves, A. 2002, ApJ, 569, L35
Ferrarese, L., & Ford, H. 2005, Space Sci. Rev., 116, 523
Ferrarese, L., & Merritt, D. 2000, ApJ, 539, L9
Gebhardt, K., et al. 2000, ApJ, 539, L13
Graham, A. 2007, preprint (astro-ph/0705.0618)
Graham, A., et al. 2001, ApJ, 563, L11
Haehnelt, M. G., & Kauffmann, G. 2000, MNRAS, 318, L35
Jørgensen, I., Chiboucas, K., Flint, K., Bergmann, M., Barr, J., & Davies, R. 2006, ApJ, 639, L9
Jørgensen, I., Franx, M., & Kjærgaard, P. 1992, A&AS, 95, 489

Kormendy, J., & Richstone, D. O. 1995, ARA&A, 33, 581
Lauer, T. R., et al. 2006, preprint (astro-ph/0606739)
Magorrian, J., et al. 1998, AJ, 115, 2285
Marconi, A., & Hunt, L. K. 2003, ApJ, 589, L21
McLure, R. J., & Dunlop, J. S. 2002, MNRAS, 331, 795
Merritt, D., & Poon, M. Y. 2004, ApJ, 606, 788
Metzroth, K. G., Onken, C. A., & Peterson, B. M. 2006, ApJ, 647, 901
Pahre, M. A., de Carvalho, R. R., & Djorgovski, S. G. 1998, AJ, 116, 1606
Sazonov, S. Yu., Ostriker, J. P., Ciotti, L., & Sunyaev, R. A. 2005, MNRAS, 358, 168
Shapiro, K. L., Cappellari, M., de Zeeuw, T., McDermid, R. M., Gebhardt, K., van den Bosch, R. C. E., & Statler, T. S. 2006, MNRAS, 370, 559
Silk, J., & Rees, M. J. 1998, A&A, 331, L1
Tonry, J. L., Dressler, A., Blakeslee, J. P., Ajhar, E. A., Fletcher, A. B., Luppino, G. A., Metzger, M. R., & Moore, C. B. 2001, ApJ, 546, 681
Tremaine, S., et al. 2002, ApJ, 574, 740